Cross-species insemination reveals mouse sperm ability to enter and cross the fish micropyle

Suma Garibova[1‡], Eva Stickler[2‡], Fatima Al Ali[1], Maha A Abdulla[1], Abbirami Sathappan[1], Sahar Da'as[1], Lilian Ghanem[2], Rick Portman[2], Matteo A Avella[1,2]*

[1]Sidra Medicine, Research Branch, Reproductive & Perinatal Health Division, Doha, Qatar; [2]Department of Biological Science, University of Tulsa, Tulsa, OK, USA.
[‡]Shared co-first authorship
*Correspondence to Matteo A Avella. **Email:** mavella@sidra.org

Author Contributions: SG, ES, FA, MAA, LG, and MAA* conceived and performed the experiments. SG, FA, AS, RP, MAA, MAA*, EV, and RP acquired images. SG and MAA* wrote the manuscript.

Competing Interest Statement: None.

Classification: Biological Sciences; Developmental Biology.

Keywords: Zona pellucida; gamete interaction; oocyte; zebrafish.

This PDF file includes:

Main Text
Figures 1 to 5
No Tables

Abstract

Extracellular matrices surrounding eggs in fish (chorion) and mammals (zona pellucida, ZP) regulate gamete recognition before fertilization, though their mechanisms differ. Mouse sperm bind and cross the ZP at any site, while fish sperm cross the chorion through a funnel-shaped opening, the micropyle. To explore these divergent processes, we established cross-species insemination assays, mixing zebrafish eggs with mouse sperm. While mouse sperm could not bind to the chorion, a subpopulation successfully located and crossed the fish micropyle. Confocal and electron microscopy revealed that sperm entered the micropyle and accumulated in the zebrafish inter-chorion space. However, transgenic mouse sperm with mCherry-labeled acrosomes failed to undergo acrosome exocytosis efficiently in the micropyle, with both acrosome-intact and reacted sperm found in the inter-chorion space. Sperm entry and crossing were dependent on the CatSper channel, as sperm from *CatSper1*^{Null} mice did not interact with or cross the micropyle. These findings suggest a conserved mechanism for sperm entry into the micropyle, providing a novel platform to investigate cross-species gamete interactions and uncover novel steps in fertilization.

Impact Statement

This study reveals that while mouse sperm cannot bind to the zebrafish chorion, a subset can enter through the micropyle in a CatSper-dependent manner, suggesting a conserved mechanism of gamete interaction across species.

Main Text

Introduction

Studies of interspecific gamete interaction have been historically important for elucidating the mechanisms regulating fertilization (VACQUIER, 1979; Vieira & Miller, 2006; Yanagimachi et al., 1976), which is required for the successful development of fish and mammals (Bhakta et al., 2019; Deneke & Pauli, 2021). Despite decades of investigation, however, the understanding of the molecular basis of sperm-egg interaction remains incomplete.

In mice, upon mating, hundreds to thousands of sperm leave the uterus and cross the uterotubal junctions, which separate the uterus from the oviduct (Avella et al., 2016; Ded et al., 2020; Suarez, 2016). These sperm bind to the epithelial cells of the isthmus in the oviduct until eggs are released from the ovary during ovulation into the ampulla of the oviduct (Hunter, 1993), where fertilization occurs. A portion of these sperm undergoes hyperactivation, which consists of a sudden change in the motility pattern of the sperm flagella, generating an asymmetrical beat that mediates the sperm release from the isthmus (Han et al., 2016). Hyperactive sperm enter the ampulla of the oviduct and traverse the cumulus mass, a hyaluronic-interspersed mass of cells, remnant of the granulosa cells from the follicle. Each cumulus mass in the ampulla may enclose a single Metaphase II (MII) egg, mature and competent for fertilization. Upon reaching the egg, sperm bind to the zona pellucida, an extracellular glycoprotein matrix composed of three glycoproteins defined as ZP1, ZP2, and ZP3. After binding, the fertilizing sperm cross the zona and fuse with the oolemma (Bhakta et al., 2019).

In fish, the sperm do not bind to the chorion surrounding the ovulated egg (Mold et al., 2001). Instead, sperm cross the chorion through a narrow, funnel-shaped canal defined as the micropyle (Yi et al., 2019). Early studies in the Pacific herring (*Clupea sp.*) show that, once released into seawater, sperm are virtually motionless until they come near the micropyle area of an egg, whereupon they become motile (Yanagimachi, 1957; Yanagimachi et al., 2017). In bitterling, zebrafish, and other fish species, sperm contact with water is sufficient to activate their motility, yet, as they pass near the micropyle area, their motility increases (Suzuki, 1958).

Because fish sperm bypass binding to the chorion using the micropyle, fish zona proteins have always been assumed to lack the ability to support sperm binding (Mold et al., 2001). Zebrafish chorion is composed of two proteins, ZP2 and ZP3, homologs to the mammalian zona proteins (Mold et al., 2001). Like other external fertilizing species, zebrafish sperm cross the chorion through the micropyle before fusing with the egg. On the other hand, mammalian eggs do not present a micropyle in the zona pellucida. Hence, sperm can cross at any binding site of the zona matrix, as shown by the presence of vesiculated acrosomal shrouds in multiple sites of the zona surface (VandeVoort et al., 1997; Wakayama et al., 1996; Yanagimachi & Phillips, 1984).

The abovementioned observations raise the predictions that mouse sperm may not recognize zebrafish ZP2 or ZP3 and would not be able to bind to the zebrafish chorion. Additionally, mouse sperm may not recognize the micropyle, as no micropyle exists in mammalian zonae pellucidae. To test these predictions, we have established a mouse-fish gamete insemination assay that consists of mixing fish eggs with mouse sperm. We show that mouse sperm could not bind to individual zebrafish ZP2/ZP3 nor to the chorion. Yet, unexpectedly, a subpopulation of mouse sperm recognized and entered the micropyle and accumulated in the oocyte inter-chorion space (ICS; the space between the inner aspects of the chorion and the oocyte). To capitalize on such discoveries, we used mouse genetics to show that only hyperactive mouse sperm could enter and cross the micropyle. We also documented that the zebrafish micropyle could not effectively induce acrosome exocytosis. Our studies provide a novel platform for cross-species insemination experiments and have implications for the mechanisms by which sperm can locate and enter micropyle of the egg.

Results

Zebrafish zona pellucida proteins are not sufficient to support mammalian sperm binding.

Zebrafish chorion is composed of two proteins defined as ZP2 and ZP3 (Mold et al., 2001). It is still unknown whether each of these two proteins individually or together can be recognized by sperm capable of binding and penetrating zona pellucidae, such as mammalian sperm. Hence, we investigated the abilities of ZP2 and ZP3 to support sperm binding by using mouse sperm. Zebrafish ZP2 isoforms present 31.09-33.09% identity to mouse ZP2 (Figure 1A). The first 6-cysteine residues of zebrafish ZP2 are organized into a trefoil domain, and zebrafish ZP2 lacks the homologous domain to the mammalian N-terminal region (Figure 1A), which has been reported to be necessary and sufficient to support mouse and human sperm binding (Avella et al., 2014; Tokuhiro & Dean, 2018). Recombinant baculovirus encoding zebrafish ZP2 and ZP3 were generated (Figure 1B). Each recombinant protein presented at the N-terminus a gp67 signal peptide from *Autographa californica* nuclear polyhedrosis virus (AcMNPV) (38 aa) to ensure proper secretion, and at the C-terminus, a 6-His tag to enable purification. Zebrafish $ZP2^{25\text{-}405}$ and $ZP3^{22\text{-}396}$ start at the N-terminus of the secreted ectodomains and include an even number of cysteine residues (Figure 1A). Confocal images and quantification with boxplots showed that mouse sperm bound sparsely to beads coated with either zebrafish ZP2 or ZP3 and to beads coated with both zebrafish ZP2 and ZP3, yet bound efficiently to beads coated with mouse ZP2 (Figure 1C and D) (Avella et al., 2016). Therefore, we could conclude that beads coated with individual zebrafish ZP2 or ZP3, or with both ZP2 and ZP3, cannot support sperm binding *in vitro* as efficiently as mouse ZP2 (Figure 1D).

Mouse sperm do not bind to the zebrafish chorion

To further validate these observations, we used native zebrafish chorion (Mold et al., 2001). First, to test whether zebrafish chorion remains intact under mouse *in vitro* fertilization (IVF) conditions, zebrafish ovulated eggs (n = 100, 3 replicates) were

incubated at 37 ^{o}C, 5% CO_2 in HTF/HSA (mouse IVF conditions) and observed over time (0, 30, 60, 120, and 240 minutes) for morphological signs of deterioration of the VE. Control eggs (n = 30, 3 replicates) were maintained in Hank's solution (Westerfield, 2007) at room temperature (Suppl. Figure 1). Under mouse IVF conditions, zebrafish oocytes presented no signs of zona deterioration within the first 60 minutes (Suppl. Figure 1). Therefore, we used 60 minutes as the time limit for incubating zebrafish chorion or eggs with mouse sperm (previously incubated for 45 min at 37 ^{o}C, 5% CO_2 in HTF/HSA).

Zebrafish ovulated eggs were collected and preserved in Hank's saline solution to prevent egg activation (Westerfield, 2007). As HTF contains water, it may induce activation of zebrafish oocytes, which may result in post-fertilization biochemical modification of the ZP proteins of the chorion (Masuda et al., 1991). Thus, we mechanically isolated the chorion from zebrafish eggs in Hank's, moved them to HTF/HSA, and inseminated them with 10^5 progressive motile mouse sperm (Figure 1E). The isolated chorion was found to not support mouse sperm binding (Figure 1F, top-left). To quantify these observations that involve gametes of considerably different sizes (~80 µm for mouse egg/2-cell embryo vs. ~700 µm for zebrafish egg), we acquired z maximum intensity projections of inseminated eggs/embryos by confocal microscopy (LSM800, Zeiss), and calculated the number of sperm bound per 20-µm^2 area using the ZEN 3.2 software (Figure 1G). Our quantitative analyses using boxplots showed that mouse sperm bind to the fish chorion (0.025 ± 0.11, s.e.m.) with significantly lower efficiency to mouse zonae (0.76 ± 0.05, s.e.m.) (Figure 1F, top-right), and with comparable efficiency to the zonae surrounding mouse 2-cell embryos (0.041 ± 0.01, s.e.m.) (Figure 1F, bottom-right).

In addition, whole ovulated zebrafish oocytes surrounded by a chorion were placed in HTF/HSA and inseminated with 10^5 progressive motile mouse sperm (37 ^{o}C, 5% CO_2 in HTF/HSA) for 60 minutes. Inseminated zebrafish oocytes showed very few sperm bound to the chorion (Figure 1F, bottom-left). Quantification of these observations found that mouse sperm bind to the chorion surrounding zebrafish eggs with comparable efficiency (0.06 ± 0.02 s.e.m.) as to the chorion only (no oocyte within) isolated from zebrafish eggs in Hank's solution (Figure 1G). From these observations, we conclude that mouse sperm cannot bind to the zebrafish VE.

Mouse sperm recognize the micropylar region of fish oocytes

Although the chorion does not support mouse sperm binding, the micropyle region of ovulated oocytes is known to attract fish sperm (Yanagimachi, 1957; Yanagimachi et al., 2013). This is due to the presence of still unidentified glycosylated protein(s) present in the micropylar region of fish eggs (Figure 2A and B). Previous literature reported contradictory findings on the absence (Yanagimachi et al., 2017) or presence (Dingare et al., 2018) of glycoprotein(s) in the zebrafish micropyle that, here, we define as the micropyle glycoprotein (MP). To test for the presence of the MP in zebrafish, we stained freshly ovulated oocytes with fluorescently conjugated wheat germ agglutinin (WGA-633). We confirmed the presence of a positive signal in the micropylar region of zebrafish oocytes (Figure 2A), as previously described (Dingare et al., 2018). Using fish

IVF conditions, we inseminated zebrafish ovulated eggs with zebrafish sperm and imaged sperm around the micropylar area and within the inner opening of the micropyle (Figure 2B). The presence of sperm after insemination was found to depend on the presence of the MP. Indeed, when the MP was biochemically removed with trypsin (Figure 2C and D), the number of zebrafish sperm surrounding the micropylar region or entering the micropyle significantly decreased (Figure 2E and F), which also led to a reduction in the fertilization rates (Figure 2G).

While performing our cross-species insemination assay, upon *in vitro* insemination of zebrafish ovulated oocytes with mouse sperm (37 ^{o}C, 5% CO_2, HTF/HSA), we could observe the accumulation of mouse sperm to the chorion area surrounding the micropyle (Figure 3A, left panel). This binding persisted after extensive washes with a glass pipette, which was able to detach loosely bound mouse sperm to mouse 2-cell embryos (negative control; Figure 1F).

To capture live mouse sperm entering the micropyle, we inseminated 20 zebrafish ovulated eggs in 300 µl HTF (Merck Millipore, USA) with 3,000 progressive motile sperm and performed 4 different independent experiments using mouse sperm from three different fertile males. Mouse sperm reached the zebrafish oocytes 48.5 ±10.6 seconds post insemination and entered the micropyle canal within 24.5 ± 7.1 seconds after approaching the zebrafish oocyte, attempting to cross the micropylar opening (Figure 3E and suppl videos 1-2).

Then, to assess the ability of the zebrafish micropyle to support mouse sperm binding independently from the oocyte, we mechanically isolated the chorion in Hank's solution to prevent oocyte activation. The micropylar region of the isolated chorion supported mouse sperm binding (Figure 3A, right panel). The binding pattern of the mouse sperm was comparable with zebrafish sperm binding around the micropyle region (Figure 2B). Upon quantification of these observations with boxplots, we found that mouse sperm bound the micropylar region (1.11 ± 0.1, s.e.m.) with comparable efficiency to mouse zonae pellucidae (1.07 ± 0.07, s.e.m.) surrounding ovulated eggs (Figure 3B). Trypsin digestion of the chorion virtually eliminated the MP as shown by the absence of WGA-633 staining (Suppl. Figure 2A). When inseminated with mouse sperm, trypsin-treated micropyle regions did not support sperm binding (Suppl. Figure 2B). From these observations, we concluded that mouse sperm can recognize the fish micropyle *in vitro*, and such recognition is dependent on the presence of the MP.

It is conceivable that, if the MP exerts a chemotactic effect on zebrafish and mouse sperm, it would be expected that this factor produces a concentration gradient. To measure if a fluorescence gradient may exist from the periphery towards the micropyle inner opening, via ImageJ/Fiji, we measured the raw integrated density (RID) (Brazill et al., 2018) of the zebrafish WGA-633-stained chorion encompassing the micropyle (n = 10) (Figure 3C). We found that fluorescence density increases from the periphery towards the central 40 µm area encompassing the micropyle region (Figure 3D, left-Y axis). Of note, we observed an increasing number of mouse sperm bound to the chorion

from the periphery towards the micropyle (Figure 3D, right-Y axis). The direct correlation between the increasing fluorescence density and the number of sperm bound from the periphery towards the micropyle is consistent with the potential role of the MP as a chemoattractant to guide sperm towards the micropyle(Yanagimachi, 1957; Yanagimachi et al., 2013).

Mouse sperm cross the fish micropyle opening

In mammalian fertilization, after binding, sperm cross the zona to enter the perivitelline space (PVS). Consequently, we aimed to study whether, after binding, mouse sperm could cross the chorion in the micropyle region. Using confocal microscopy (Zeiss LSM 800), we found that multiple mouse sperm entered the micropyle canal and crossed the micropyle opening, accumulating in the ICS (Figure 3A; n = 12-14 eggs, 3 replicates). After crossing, sperm concentrated either around the micropyle region (Figure 3A left and mid panels) or away from the micropyle (Figure 3A, right panel). Quantifications of these observations revealed a comparable, yet significantly higher, number of ICS mouse sperm around the micropyle than away from the micropyle (Figure 3B).

We, then, wondered at what site of the micropyle region mouse sperm crossed the VE. Previous studies have shown that, after zona binding, mammalian sperm can cross the matrix at any binding site (VandeVoort et al., 1997; Wakayama et al., 1996; Yanagimachi & Phillips, 1984), whereas fish sperm cross the chorion only at the micropyle inner opening (Yi et al., 2019). Thus, we investigated whether mouse sperm cross the chorion at any site of the micropyle region or, like fish sperm, use the inner opening of the micropyle. Using scanning electron microscopy (SEM), we observed mouse sperm within the micropyle canal (Figure 3C, left). However, no mouse sperm were found mid-way through the chorion in the micropyle region, indicating that mouse sperm, likely, used the micropyle inner opening to cross the fish VE. To validate this thesis, we used transmission electron microscopy (TEM) to study mouse sperm in the micropyle canal (Figure 3C, mid and right). TEM analyses confirmed that mouse sperm did not cross the chorion at the binding site. From this, we concluded that the interaction between mouse sperm and the zebrafish micropyle may differ from the mechanism of sperm binding with the zona pellucida. To that end, we used sperm from transgenic mice to further characterize the nature of this interaction.

Ineffective induction of mouse sperm acrosome exocytosis during interaction with the fish micropyle

The acrosome is present in the sperm of only a few chondrostean species, such as the sturgeon fish. In these species, sperm undergo acrosome exocytosis in the micropyle canal (Psenicka et al., 2010). Sperm from teleost fish species like zebrafish, however, lack an acrosome. Thus, one may hypothesize that the zebrafish micropyle lacks the ability to induce acrosome exocytosis (Hirohashi & Yanagimachi, 2018).

To determine whether the zebrafish micropyle can induce mouse sperm acrosome exocytosis, we used TEM and confocal microscopy to track the status of the acrosomes of mouse spermatozoa during cross-species insemination. We used transgenic mouse

sperm that accumulate mCherry in the acrosome (Avella et al., 2016) (*Acrosin*^{Tg}). Acrosome-intact sperm present a visible fluorescent acrosome beneath the nucleus (Avella et al., 2016). During acrosome exocytosis, mCherry is released upon fusion of the sperm plasma membrane with the outer acrosomal membrane (7). This results in the loss of fluorescent signal and marks these sperm as 'acrosome-reacted', as documented by fluorescent and electron microscopy analyses (Avella et al., 2016). Through confocal microscopy, we found 86 ± 4 % (n = 10, s.e.m) of sperm surrounding the micropyle to be acrosome intact (Figure 3D and E). Sperm could cross the micropyle inner opening irrespective of their acrosomal status (reacted or intact; Figure 3C, mid and right, respectively). Additionally, both acrosome-intact and acrosome-reacted sperm were found in the ICS via confocal and TEM (Figure 3F). Thus, we concluded that mouse sperm can recognize the micropylar region of zebrafish oocytes and cross the micropyle inner opening regardless of the acrosome status, though passage through the micropyle does not appear to induce acrosome exocytosis.

Mouse CatSper is necessary to mediate sperm crossing the zebrafish micropyle.

We found that mouse sperm in the fish ICS were still motile and presenting what may appear to be a hyperactive motility pattern (Supplementary Videos 3-5). To test whether mouse sperm entering and crossing the micropyle depends on hyperactive motility, we inseminated zebrafish eggs with *CatSper1*^{Null} sperm. The sperm of *CatSper1*^{Null} mice lack the CatSper channel and cannot undergo hyperactivation, which results in failure of *CatSper1*^{Null} sperm to fertilize eggs (Ren et al., 2001a).

First, we quantified the ability of *CatSper1*^{Null} sperm to bind to mouse zonae pellucidae *in vitro* or to cross the zonae pellucidae *in vivo* under our experimental conditions. To quantify the ability of *CatSper1*^{Null} sperm to bind to the zona matrix, we incubated sperm from infertile *CatSper1*^{Null} males (no sired pups after mating for 1.5 months with fertile females) or fertile *CatSper1*^{Het} males (≥1 litter sired after mating with fertile females for 1.5 months) for 45 min in HTF/HSA, 37 ^{o}C, 5% CO_2, and used either mutant sperm to separately inseminate fertile ovulated MII eggs that were previously denuded from cumulus masses by hyaluronidase (16-22 eggs, 3 replicates). We found that *CatSper1*^{Null} sperm bound to mouse zonae with comparable efficiency (60.2 ± 3.55; s.e.m.) to *CatSper1*^{Het} sperm (66.5 ± 1.26, s.e.m) (Figure 4A and B). To quantify the ability of *CatSper1*^{Null} sperm to cross the zona, we mated five *CatSper1*^{Null} or *CatSper1*^{Het} males with five *Cd9*^{Null} females, whose eggs rarely fuse with sperm, leading to an accumulation of supernumerary sperm in the PVS. We found that *Cd9*^{Null} eggs from females mated with *CatSper1*^{Het} males accumulated 4.1 ± 1.57 (s.e.m.) in the PVS, whereas there were no sperm detected in the *Cd9*^{Null} eggs from females mated with *CatSper1*^{Null} males (10 females, 10-15 eggs/female) (Figure 4C and D). These data confirmed the inability of *CatSper1*^{Null} sperm to cross the zona *in vivo* and are consistent with previous reports showing *CatSper1*^{Null} sperm being unable to fertilize eggs under *in vivo* conditions (Ren et al., 2001a).

To see whether the CatSper channel is necessary for the mouse sperm to enter and cross the zebrafish micropyle, we inseminated zebrafish eggs with *CatSper1*^{Null} or *CatSper1*^{Het}

sperm. We rarely found *CatSper1*^{Null} sperm in the micropyle of zebrafish eggs and never found *CatSper1*^{Null} sperm in the fish PVS, indicating that CatSper is necessary for mouse sperm to enter cross the micropyle (Figure 4E and F).

Discussion

By establishing a mouse-fish gamete interaction assay, we report that, although the chorion cannot support mouse sperm binding, a subpopulation of mouse sperm can find and enter the fish micropyle. Mouse sperm cross the micropyle and accumulate in the fish PVS. Using sperm from different transgenic mouse lines, we found that the recognition of the micropyle by mouse sperm is dependent on the CatSper channel and that the zebrafish micropyle failed to effectively induce acrosome exocytosis.

By Clustal Ω sequence alignment (Sievers et al., 2011), it appears that zebrafish zona proteins lack an N-terminal domain with conserved sequence identity to the mammalian ZP2 N-terminus (Avella et al., 2014). Therefore, the observed absence of mouse sperm binding to zebrafish ZP2 or the chorion is consistent with a model that envisions the N-terminal region of mammalian ZP2 to be required for mouse sperm binding to an extracellular matrix (Avella et al., 2014; Bhakta et al., 2019).

The ability of sperm to effectively localize eggs is vital for external fertilizing species that emit their gametes in the water column. In sea urchins, small peptides such as Resact have been identified as the molecule mediating the sperm attracting stimulus to the unfertilized egg. In zebrafish, and other teleost fish species, sperm contact with water is sufficient to activate their motility, yet as they pass near the micropyle area, their motility increases (Suzuki, 1958). Such a gain in motility appears to be elicited by exposure to the MP that guides the fertilizing sperm into the micropyle (Yanagimachi et al., 1992). We and others have shown that removal of the MP by trypsin digestion significantly decreases egg fertilization rate, indicating the important role of MP in fish fertilization (Yanagimachi et al., 2013). Sea urchin Resact induces a cGMP signaling pathway that mediates Ca^{2+} bursts via the CatSper channel, and the increased cytoplasmic Ca^{2+}concentrations confer sperm chemotactic steering towards the egg (Seifert et al., 2015). In addition, it has been hypothesized that the fish CatSper channel may also play a role in activating fish sperm motility during fertilization (Yanagimachi et al., 2017). Upon binding with motile sperm, the MP may activate sperm proton pumps, leading to an increase in intracellular pH; this, in turn, would activate CatSper channels, resulting in a Ca^{2+} influx and higher levels of intracellular Ca^{2+}. Higher concentrations of intracellular Ca^{2+} would make the sperm tail beating pattern change from symmetrical to asymmetrical, directing sperm entry into the micropyle (Yanagimachi et al., 2017). Consistent with these hypotheses, our data demonstrates that CatSper is necessary to mediate mouse sperm entering and crossing the zebrafish micropyle. Like fish sperm, it is conceivable that the MP may elicit an attractant stimulus towards a subpopulation of mouse sperm. However, recent findings have shown successful cross-species fertilization of evolutionary-distant fish species, such as with female common carp and male blunt

snout bream (S. Wang et al., 2017) or Russian Sturgeon with American Paddlefish (Káldy et al., 2020), suggesting that such a stimulus may not act with species-specificity. This is consistent with findings that show how sperm from other fish species (Yanagimachi et al., 2013, 2017) may reach and cross the micropyle of different fish species (Yanagimachi et al., 2017).

The potential existence of a mammalian sperm chemoattraction mechanism has been the focus of considerable research efforts. Using *in vitro* assays to quantify chemoattraction in mammalian sperm (e.g., Zigmond chamber), several studies have shown evidence of a putative attraction mechanism coming from the egg microenvironment (Eisenbach & Giojalas, 2006), with subpopulations of sperm that responded to chemical gradients obtained from egg extracts or oviductal fluids (Fabro et al., 2002; Giojalas & Rovasio, 1998; Oliveira et al., 1999; Sun et al., 2005). However, no follow-up studies with genetic loss-of-function assays could characterize such a mechanism further. Hence, it is still uncertain whether mammalian sperm may respond to attracting stimuli from an egg (Yanagimachi, 2022). Our data suggests the presence of a conserved mechanism that attracts mouse sperm towards eggs. Although such stimulus comes from a fish egg, it is plausible to reason that a mammalian protein homologous to the fish MP may play a similar role towards a subpopulation of mouse sperm that swim near an ovulated egg in the ampulla. Unfortunately, studies using mass spectrometry, together with cloning, immunohistochemistry, and in situ hybridization, were unable to identify the nature of the fish MP (Oda et al., 1995, 1998; Vines et al., 2002, p. 202). Therefore, this factor is still unidentified.

To successfully fertilize an egg, mammalian sperm must undergo acrosome exocytosis, as only acrosome-reacted sperm can fuse with the oolemma (Bhakta et al., 2019). Typically, fish sperm do not present an acrosome. However, in fish species whose sperm do possess an acrosome, such as sturgeon (Psenicka et al., 2010), exocytosis occurs as sperm migrate into the micropyle prior to fusion with the egg (Alavi et al., 2012; Psenicka et al., 2010). Zebrafish are teleost and do not develop spermatozoa with acrosomes. In our studies, mouse sperm found in the micropyle or the PVS of zebrafish eggs were often observed to be acrosome-intact. Failed acrosome exocytosis has been observed in previous cross-species insemination studies in rodents, where sperm could penetrate zonae of different species while remaining acrosome-intact (VandeVoort et al., 1997; Wakayama et al., 1996; Yanagimachi & Phillips, 1984), indicating putative species-specific oocyte mechanisms of induction of acrosome exocytosis (Avella & Dean, 2011). As zebrafish sperm do not present an acrosome, it is conceivable that, unlike sturgeon, zebrafish oocytes may lack the ability to induce acrosome exocytosis in the micropyle.

In conclusion, the existence of a MP mediating fish and mouse sperm raises the prediction for the potential existence of a mouse ortholog for the fish MP and of a cognate sperm receptor. Future studies will focus on identifying the fish MP, looking for mammalian orthologs, and characterizing its expression during fish and mouse oogenesis.

In addition, mutant-null fish or mouse models will aid in characterizing the role(s) of these proteins in regulating fish and mouse fertilization.

Materials and Methods

IACUC sentence

Experiments with zebrafish (AB line) or normal and transgenic mice were performed in compliance with the guidelines of the Animal Care and Use Committee of Sidra Medicine and the University of Tulsa under the approved animal study protocols, Sidra Medicine IACUC 2204916, and University of Tulsa TU-0050 and TU-0050R1

Genotyping

Transgenic mice were genotyped by PCR ([95°C for 30 s, 56°C for 30 s, 72°C for 1 min] × 30 cycles, 72°C for 7 min, and 4°C for >30 min) using primers from previous publications *Acr*^{Tg} (Avella et al., 2016), *CatSper1*^{Null} (Ren et al., 2001b), and *Cd9*^{Null} (Le Naour et al., 2000, p. 9).

Light microscopy

Samples were mounted in PBS, and images of oocytes, embryos, and beads were acquired with a dissecting microscope SMZ-2B (Nikon, Japan) at 5X magnification, with an inverted microscope ECLIPSE TS100 (Nikon) or with a confocal microscope (LSM 800, Zeiss) using 10X or 20X objective lens at room temperature (Avella et al., 2014). Using ZEN 3.2 image software (Zeiss), LSM 800 images were exported as 300 dpi resolution TIF files and combined using Adobe Illustrator 25.0. Alternatively, maximum intensity projections of confocal optical sections to a single plane were acquired and merged with DIC images of oocytes, embryos, or agarose beads.

Electron microscopy

Zebrafish oocytes inseminated with mouse sperm were fixed in 2% glutaraldehyde in 0.1 M cacodylate buffer (pH 7.4) and incubated at 4°C for 2 hours. After a series of washes in cacodylate buffer, the eggs were embedded in 2% agarose. The samples were dehydrated through a graded series of ethanol and processed for embedding in LR White resin. Ultrathin sections were obtained with an ultramicrotome (Microm International GmbH) and mounted on formvar-coated nickel grids (Electron Microscopy Sciences). Ultrathin sections were counterstained with uranyl acetate followed by lead citrate and imaged in a Jeol JEM-1011 transmission electron microscope (Jeol).

Expression of recombinant zebrafish ZP2 and ZP3

cDNA encoding zebrafish ZP2 (AAK16577.1; 25-405 aa) and ZP3 (NP_571406; 22-396 aa) (H. Wang & Gong, 1999) were cloned into pFastBac-HBM TOPO (Invitrogen) downstream of a polyhedron promoter and a gp67 signal peptide from *Autographa californica* nuclear polyhedrosis virus (AcMNPV) (38 aa). At the 3' end of the open reading frame, each clone carried a 6-His tag encoded in frame to enable peptide purification. Bacmid DNA, isolated after transformation into DH10Bac *Escherichia coli*, was used to transfect insect cells to produce recombinant baculovirus particles for

infection of *Sf9* cells using manufacturer protocols (Genscript). Recombinant peptides were purified on IMAC Sepharose High-Performance beads (Cytiva) per manufacturer instructions and assayed on SDS-PAGE as previously reported (Avella et al., 2014). Plasmid cloning and peptide expression were performed by Genscript (USA).

Mouse gamete collection and *in vitro* insemination

Female mice were stimulated with 5 IU of equine chorionic gonadotropin (eCG) (ProspecBio) and 48 hrs later with human chorionic gonadotropin (hCG) (Sigma-Aldrich). Twelve hours after hCG injection, eggs in cumulus were collected and incubated (37 ^{o}C, 5% CO_2) in HTF/HSA under mineral oil before insemination with mouse sperm. Alternatively, eggs were denuded from the cumulus mass with hyaluronidase (Millipore) and washed in HTF/HSA before insemination with mouse sperm. Fertilization was scored 24 hours post-insemination by quantifying the number of two-cell embryos. To assess *in vivo* female fertility, mutant female mice (n $\geq$3) were co-caged with one control fertile female and one fertile male mouse, and litters were recorded until females gave birth to at least three litters.

Epididymal sperm from 10-14 weeks old male mice were incubated under capacitating conditions in human tubal fluid (HTF) supplemented with 0.4% Human Serum Albumin (HSA; Cooper Surgical) for 45 min (37 ^{o}C, 5% CO_2) (Avella et al., 2014). Sperm were added to oocytes or embryos in 50 µl of HTF/HSA drops under mineral oil at a final concentration of 10^5/ml progressive motile sperm quantified by hemocytometer. Upon coincubation, inseminated oocytes/embryos were washed by gently pipetting with a 200 µl microcapillary pipette (Cooper Surgical) to remove loosely bound sperm. Samples were, then, fixed in 2% paraformaldehyde and stained with Hoechst and WGA-633 (ThermoFisher) to identify the nuclei and the glycoproteins of the zona pellucidae. To assess mouse sperm binding, mouse eggs and two-cell embryos were used as positive and negative controls, respectively.

Zebrafish gamete collection and *in vitro* insemination

Zebrafish females or males (separated from tank mates the night prior) were anesthetized with tricaine (3-amino benzoic acidethylester) solution (Sigma). After being gently dried with a kimwipe, each female was moved to a dry petri dish, and mild pressure on the fish belly was applied, stroking from anterior to posterior. Released oocytes were separated from the female using flat forceps and inseminated with zebrafish sperm. Alternatively, zebrafish oocytes were preserved in Hank's saline (Westerfield, 2007) and, then, were gently acclimated to HTF/HSA (Cooper Surgical) and inseminated with mouse sperm previously incubated under capacitating conditions (HTF/HSA, 37 ^{o}C, 5% CO_2) (Avella et al., 2014). Before insemination with mouse sperm, zebrafish oocytes were, in some instances, treated with 0.001% trypsin (crystalline, VWR) in Ringer's solution (Westerfield, 2007) for 1 – 5 min, and rinsed twice in Hank's solution before cross-species insemination (HTF/HSA, 37 ^{o}C, 5% CO_2). Zebrafish oocytes and mouse sperm were incubated for 60 min (HTF/HSA, 37 ^{o}C, 5% CO_2), washed in HTF/HSA to remove loosely bound sperm, and then fixed in 2% paraformaldehyde. Zebrafish males were dried with a kimwipe, and both sides of the body were firmly stroked to collect sperm out

of their genital pore with a microcapillary pipette (Cooper Surgical). Sperm were preserved in ice-cold, full-strength Hank's saline until oocyte insemination (Westerfield, 2007). Upon oocyte insemination, samples were immediately fixed in 2% paraformaldehyde and stained with Hoechst and Wheat Germ Agglutinin, Alexa Fluor™ 633 Conjugate (WGA-633, ThermoFisher) to identify the nuclei and the micropyle, respectively. Fluorescence intensity of the micropyle was measured as Raw integrated density using Fiji/ImageJ (Brazill et al., 2018).

Live imaging of mouse sperm attraction to the micropyle of zebrafish mature eggs

Ovulated zebrafish oocytes were collected, acclimated as described above, and immediately transferred to the imaging dish containing 300 µl of HTF/BSA under mineral oil. The micropyle area was identified and brought into focus. Mouse sperm, collected and capacitated as previously described, were prepared for imaging. Images were captured using an inverted microscope (Nikon Eclipse Ti) equipped with a 12MP camera. After focusing on the micropyle, 3,000 progressively motile sperm were introduced into the imaging dish, and time-lapse live imaging was performed to record gamete interactions.

Gamete or embryo quantifications and statistics

Mouse sperm bound to oocytes or beads were quantified from z maximum intensity projections obtained by confocal microscopy (LSM800, Zeiss). The number of sperm bound per mouse oocyte/embryo or per 20-μm^2 area (mouse and zebrafish oocytes/embryos) was obtained using the ZEN 3.2 software (Blue Edition, Zeiss). Descriptive statistics were used for comparisons of mouse sperm bound to oocytes, embryos, or agarose beads and for mouse sperm that have crossed the zonae with One-Way ANOVA followed by Tukey HSD (honestly significant difference) post-hoc test analyses. The number of sperm was represented as bars or boxplots reflecting the median (horizontal line) and data points within the 10th and 90th percentiles (error bars) for at least three independent experiments. Boxes included the middle two quartiles, and outliers, when present, were indicated by dots. All statistical analyses were performed using R Studio (v. 3.6.3).

Acknowledgments

We thank Drs. Andrea Pauli and Masahito Ikawa for the critical reading of the manuscript, and Dr. Jean-Ju Chung for the *CatSper1*^{Null} mice. We are grateful to Billi Bobala and Lucas Cline for their assistance during the experiments.

Funding

This study was supported by the:

Sidra Medicine grant SDR400185

University of Tulsa, Department of Biological Science, Office of Research and Sponsored Programs (Faculty Research Grant and Faculty Research Summer Fellowship) to MA
University of Tulsa, the Tulsa Undergraduate Research Challenge (TURC) program to ES and LG.

References

Alavi, S. M. H., Hatef, A., Pšenička, M., Kašpar, V., Boryshpolets, S., Dzyuba, B., Cosson, J., Bondarenko, V., Rodina, M., Gela, D., & Linhart, O. (2012). Sperm biology and control of reproduction in sturgeon: (II) sperm morphology, acrosome reaction, motility and cryopreservation. *Reviews in Fish Biology and Fisheries*, *22*(4), 861–886. https://doi.org/10.1007/s11160-012-9270-x

Avella, M. A., Baibakov, B. A., Jimenez-Movilla, M., Sadusky, A. B., & Dean, J. (2016). ZP2 peptide beads select human sperm in vitro, decoy mouse sperm in vivo, and provide reversible contraception. *Science Translational Medicine*, *8*(336), 336ra60. https://doi.org/10.1126/scitranslmed.aad9946

Avella, M. A., Baibakov, B., & Dean, J. (2014). A single domain of the ZP2 zona pellucida protein mediates gamete recognition in mice and humans. *The Journal of Cell Biology*, *205*(6), 801–809. https://doi.org/10.1083/jcb.201404025

Avella, M. A., & Dean, J. (2011). Fertilization with acrosome-reacted mouse sperm: Implications for the site of exocytosis. *Proceedings of the National Academy of Sciences*, *108*(50), 19843–19844. https://doi.org/10.1073/pnas.1118234109

Bhakta, H. H., Refai, F. H., & Avella, M. A. (2019). The molecular mechanisms mediating mammalian fertilization. *Development*, *146*(15), dev176966. https://doi.org/10.1242/dev.176966

Brazill, J. M., Zhu, Y., Li, C., & Zhai, R. G. (2018). Quantitative Cell Biology of Neurodegeneration in Drosophila Through Unbiased Analysis of Fluorescently Tagged Proteins Using ImageJ. *Journal of Visualized Experiments : JoVE*, *138*, 58041. https://doi.org/10.3791/58041

Ded, L., Hwang, J. Y., Miki, K., Shi, H. F., & Chung, J.-J. (2020). 3D in situ imaging of the female reproductive tract reveals molecular signatures of fertilizing spermatozoa in mice. *eLife*, *9*. https://doi.org/10.7554/eLife.62043

Deneke, V. E., & Pauli, A. (2021). The Fertilization Enigma: How Sperm and Egg Fuse. *Annual Review of Cell and Developmental Biology*, *37*, 391–414. https://doi.org/10.1146/annurev-cellbio-120219-021751

Dingare, C., Niedzwetzki, A., Klemmt, P. A., Godbersen, S., Fuentes, R., Mullins, M. C., & Lecaudey, V. (2018). The Hippo pathway effector Taz is required for cell morphogenesis and fertilization in zebrafish. *Development (Cambridge, England)*, *145*(22). https://doi.org/10.1242/dev.167023

Eisenbach, M., & Giojalas, L. C. (2006). Sperm guidance in mammals—An unpaved road to the egg. *Nature Reviews. Molecular Cell Biology*, *7*(4), 276–285. https://doi.org/10.1038/nrm1893

Fabro, G., Rovasio, R. A., Civalero, S., Frenkel, A., Caplan, S. R., Eisenbach, M., & Giojalas, L. C. (2002). Chemotaxis of Capacitated Rabbit Spermatozoa to Follicular Fluid Revealed by a Novel Directionality-Based Assay1. *Biology of Reproduction*, *67*(5), 1565–1571. https://doi.org/10.1095/biolreprod.102.006395

Giojalas, L. C., & Rovasio, R. A. (1998). Mouse spermatozoa modify their motility parameters and chemotactic response to factors from the oocyte microenvironment. *International Journal of Andrology*, *21*(4), 201–206.

Han, L., Nishimura, K., Sadat Al Hosseini, H., Bianchi, E., Wright, G. J., & Jovine, L. (2016). Divergent evolution of vitamin B9 binding underlies Juno-mediated adhesion of mammalian gametes. *Current Biology: CB*, *26*(3), R100-101. https://doi.org/10.1016/j.cub.2015.12.034

Hirohashi, N., & Yanagimachi, R. (2018). Sperm acrosome reaction: Its site and role in fertilization. *Biology of Reproduction*, *99*(1), 127–133. https://doi.org/10.1093/biolre/ioy045

Hunter, R. H. (1993). Sperm:egg ratios and putative molecular signals to modulate gamete interactions in polytocous mammals. *Molecular Reproduction and Development*, *35*(3), 324–327. https://doi.org/10.1002/mrd.1080350315

Káldy, J., Mozsár, A., Fazekas, G., Farkas, M., Fazekas, D. L., Fazekas, G. L., Goda, K., Gyöngy, Z., Kovács, B., Semmens, K., Bercsényi, M., Molnár, M., & Patakiné Várkonyi, E. (2020). Hybridization of Russian Sturgeon (Acipenser gueldenstaedtii, Brandt and Ratzeberg, 1833) and American Paddlefish (Polyodon spathula, Walbaum 1792) and Evaluation of Their Progeny. *Genes*, *11*(7). https://doi.org/10.3390/genes11070753

Le Naour, F., Rubinstein, E., Jasmin, C., Prenant, M., & Boucheix, C. (2000). Severely reduced female fertility in CD9-deficient mice. *Science (New York, N.Y.)*, *287*(5451), 319–321.

Masuda, K., Luchi, I., & Yamagami, K. (1991). Analysis of Hardening of the Egg Envelope (Chorion) of the Fish, Oryzias latipes. *Development, Growth & Differentiation*, *33*(1), 75–83. https://doi.org/10.1111/j.1440-169X.1991.00075.x

Mold, D. E., Kim, I. F., Tsai, C. M., Lee, D., Chang, C. Y., & Huang, R. C. (2001). Cluster of genes encoding the major egg envelope protein of zebrafish. *Molecular Reproduction and Development*, *58*(1), 4–14. https://doi.org/10.1002/1098-2795(200101)58:1<4::AID-MRD2>3.0.CO;2-P

Oda, S., Igarashi, Y., Manaka, K., Koibuchi, N., Sakai-Sawada, M., Sakai, K., Morisawa, M., Ohtake, H., & Shimizu, N. (1998). Sperm-Activating Proteins Obtained from the Herring Eggs Are Homologous to Trypsin Inhibitors and Synthesized in Follicle Cells. *Developmental Biology*, *204*(1), 55–63. https://doi.org/10.1006/dbio.1998.9056

Oda, S., Igarashi, Y., Ohtake, H., Sakai, K., Shimizu, N., & Morisawa, M. (1995). Sperm-activating proteins from unfertilized eggs of the Pacific herring, Clupea pallasii. *Development, Growth & Differentiation*, *37*(3), 257–261. https://doi.org/10.1046/j.1440-169X.1995.t01-2-00003.x

Oliveira, R. G., Tomasi, L., Rovasio, R. A., & Giojalas, L. C. (1999). Increased velocity and induction of chemotactic response in mouse spermatozoa by follicular and

oviductal fluids. *Reproduction*, *115*(1), 23–27. https://doi.org/10.1530/jrf.0.1150023

Psenicka, M., Rodina, M., & Linhart, O. (2010). Ultrastructural study on the fertilisation process in sturgeon (Acipenser), function of acrosome and prevention of polyspermy. *Animal Reproduction Science*, *117*(1–2), 147–154. https://doi.org/10.1016/j.anireprosci.2009.03.013

Ren, D., Navarro, B., Perez, G., Jackson, A. C., Hsu, S., Shi, Q., Tilly, J. L., & Clapham, D. E. (2001a). A sperm ion channel required for sperm motility and male fertility. *Nature*, *413*(6856), Article 6856. https://doi.org/10.1038/35098027

Ren, D., Navarro, B., Perez, G., Jackson, A. C., Hsu, S., Shi, Q., Tilly, J. L., & Clapham, D. E. (2001b). A sperm ion channel required for sperm motility and male fertility. *Nature*, *413*(6856), 603–609. https://doi.org/10.1038/35098027

Seifert, R., Flick, M., Bönigk, W., Alvarez, L., Trötschel, C., Poetsch, A., Müller, A., Goodwin, N., Pelzer, P., Kashikar, N. D., Kremmer, E., Jikeli, J., Timmermann, B., Kuhl, H., Fridman, D., Windler, F., Kaupp, U. B., & Strünker, T. (2015). The CatSper channel controls chemosensation in sea urchin sperm. *The EMBO Journal*, *34*(3), 379–392. https://doi.org/10.15252/embj.201489376

Sievers, F., Wilm, A., Dineen, D., Gibson, T. J., Karplus, K., Li, W., Lopez, R., McWilliam, H., Remmert, M., Söding, J., Thompson, J. D., & Higgins, D. G. (2011). Fast, scalable generation of high-quality protein multiple sequence alignments using Clustal Omega. *Molecular Systems Biology*, *7*, 539. https://doi.org/10.1038/msb.2011.75

Suarez, S. S. (2016). Mammalian Sperm Interactions with the Female Reproductive Tract. *Cell and Tissue Research*, *363*(1), 185–194. https://doi.org/10.1007/s00441-015-2244-2

Sun, F., Bahat, A., Gakamsky, A., Girsh, E., Katz, N., Giojalas, L. C., Tur-Kaspa, I., & Eisenbach, M. (2005). Human sperm chemotaxis: Both the oocyte and its surrounding cumulus cells secrete sperm chemoattractants. *Human Reproduction*, *20*(3), 761–767. https://doi.org/10.1093/humrep/deh657

Suzuki, R. (1958). Sperm Activation and Aggregation During Fertilization in Some Fishes. *Embryologia*, *4*(2), 93–102. https://doi.org/10.1111/j.1440-169X.1958.tb00149.x

Tokuhiro, K., & Dean, J. (2018). Glycan-Independent Gamete Recognition Triggers Egg Zinc Sparks and ZP2 Cleavage to Prevent Polyspermy. *Developmental Cell*, *46*(5), 627-640.e5. https://doi.org/10.1016/j.devcel.2018.07.020

VACQUIER, V. D. (1979). The Interactions of Sea Urchin Gametes During Fertilization. *American Zoologist*, *19*(3), 839–849. https://doi.org/10.1093/icb/19.3.839

VandeVoort, C. A., Yudin, A. I., & Overstreet, J. W. (1997). Interaction of Acrosome-Reacted Macaque Sperm with the Macaque Zona Pellucida. *Biology of Reproduction*, *56*(5), 1307–1316. https://doi.org/10.1095/biolreprod56.5.1307

Vieira, A., & Miller, D. J. (2006). Gamete interaction: Is it species-specific? *Molecular Reproduction and Development*, *73*(11), 1422–1429. https://doi.org/10.1002/mrd.20542

Vines, C. A., Yoshida, K., Griffin, F. J., Pillai, M. C., Morisawa, M., Yanagimachi, R., & Cherr, G. N. (2002). Motility initiation in herring sperm is regulated by reverse

sodium-calcium exchange. *Proceedings of the National Academy of Sciences*, *99*(4), 2026–2031.

Wakayama, T., Ogura, A., Suto, J., Matsubara, Y., Kurohmaru, M., Hayashi, Y., & Yanagimachi, R. (1996). Penetration by field vole spermatozoa of mouse and hamster zonae pellucidae without acrosome reaction. *Reproduction*, *107*(1), 97–102. https://doi.org/10.1530/jrf.0.1070097

Wang, H., & Gong, Z. (1999). Characterization of two zebrafish cDNA clones encoding egg envelope proteins ZP2 and ZP3. *Biochimica Et Biophysica Acta*, *1446*(1–2), 156–160.

Wang, S., Ye, X., Wang, Y., Chen, Y., Lin, B., Yi, Z., Mao, Z., Hu, F., Zhao, R., Wang, J., Zhou, R., Ren, L., Yao, Z., Tao, M., Zhang, C., Xiao, J., Qin, Q., & Liu, S. (2017). A new type of homodiploid fish derived from the interspecific hybridization of female common carp × male blunt snout bream. *Scientific Reports*, *7*(1), Article 1. https://doi.org/10.1038/s41598-017-04582-z

Westerfield, M. (2007). *The zebrafish book: A guide for the laboratory use of zebrafish (Danio rerio)* (5th ed.). The University of Oregon Press.

Yanagimachi, R. (1957). *Some properties of the sperm-activating factor in the micropyle area of the herring egg*. *30*, 114–119.

Yanagimachi, R. (2022). Mysteries and unsolved problems of mammalian fertilization and related topics. *Biology of Reproduction*, *106*(4), 644–675. https://doi.org/10.1093/biolre/ioac037

Yanagimachi, R., Cherr, G., Matsubara, T., Andoh, T., Harumi, T., Vines, C., Pillai, M., Griffin, F., Matsubara, H., Weatherby, T., & Kaneshiro, K. (2013). Sperm attractant in the micropyle region of fish and insect eggs. *Biology of Reproduction*, *88*(2), 47. https://doi.org/10.1095/biolreprod.112.105072

Yanagimachi, R., Cherr, G. N., Pillai, M. C., & Baldwin, J. D. (1992). Factors Controlling Sperm Entry into the Micropyles of Salmonid and Herring Eggs. *Development, Growth & Differentiation*, *34*(4), 447–461. https://doi.org/10.1111/j.1440-169X.1992.00447.x

Yanagimachi, R., Harumi, T., Matsubara, H., Yan, W., Yuan, S., Hirohashi, N., Iida, T., Yamaha, E., Arai, K., Matsubara, T., Andoh, T., Vines, C., & Cherr, G. N. (2017). Chemical and physical guidance of fish spermatozoa into the egg through the micropyle,. *Biology of Reproduction*, *96*(4), 780–799. https://doi.org/10.1093/biolre/iox015

Yanagimachi, R., & Phillips, D. M. (1984). The status of acrosomal caps of hamster spermatozoa immediately before fertilization in vivo. *Gamete Research*, *9*(1), 1–19. https://doi.org/10.1002/mrd.1120090102

Yanagimachi, R., Yanagimachi, H., & Rogers, B. J. (1976). The use of zona-free animal ova as a test-system for the assessment of the fertilizing capacity of human spermatozoa. *Biology of Reproduction*, *15*(4), 471–476. https://doi.org/10.1095/biolreprod15.4.471

Yi, X., Yu, J., Ma, C., Dong, G., Shi, W., Li, H., Li, L., Luo, L., Sampath, K., Ruan, H., & Huang, H. (2019). The effector of Hippo signaling, Taz, is required for formation of the micropyle and fertilization in zebrafish. *PLoS Genetics*, *15*(1), e1007408. https://doi.org/10.1371/journal.pgen.1007408

721
722

Figures and Tables

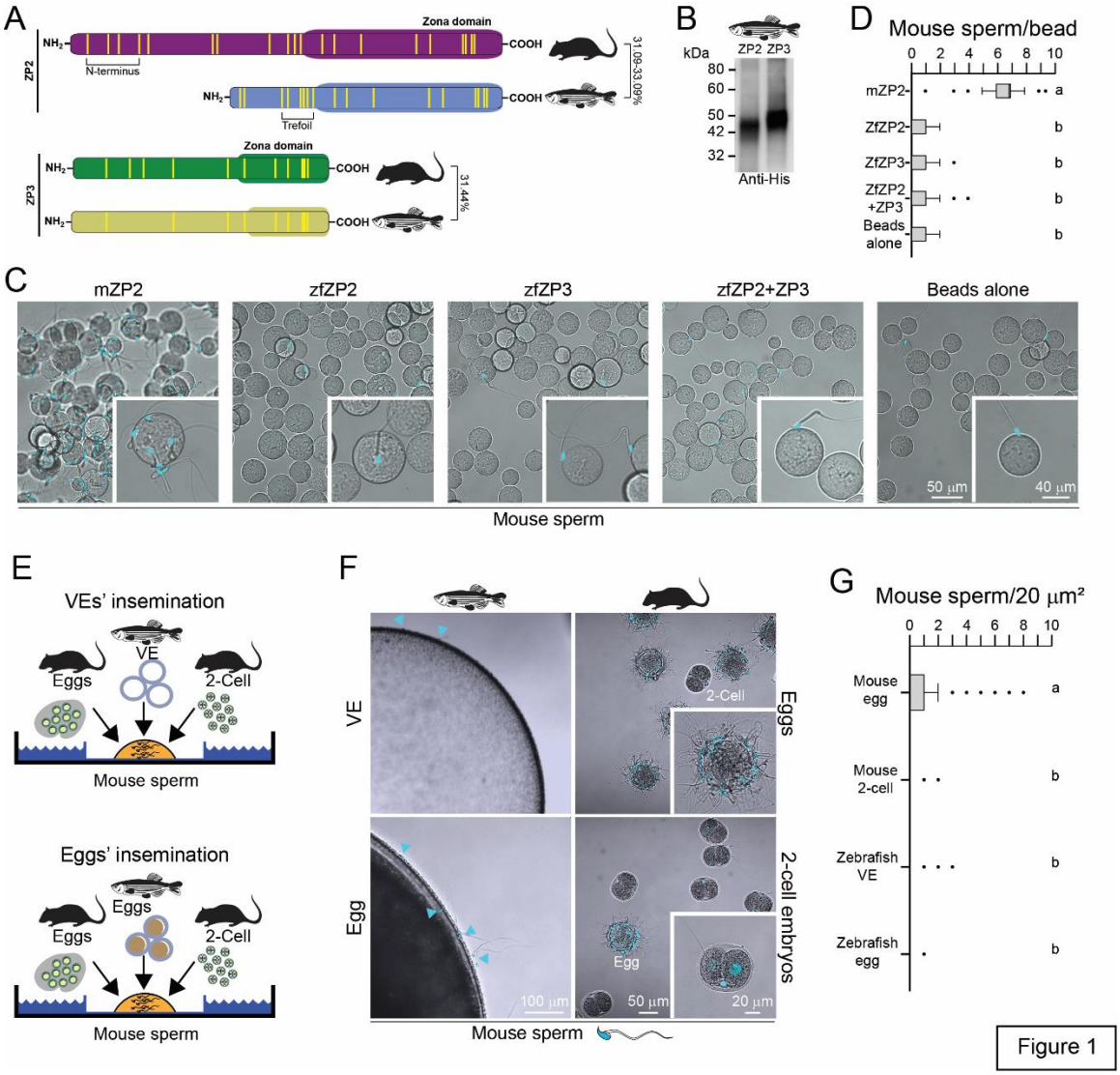

Figure 1. Mouse sperm do not bind to zebrafish zona proteins. A) Schematic of zebrafish ZP2 and ZP3 peptides compared to mammalian homologs (Clustal **Ω**). Yellow bars represent cysteine residues. Percent values indicate identity between mouse and zebrafish amino acid sequences (NP_035905.1, mouse ZP2; AAK16578.1, zebrafish ZP2, variant A; AAK16577.1, zebrafish ZP2, variant B; AAK16579.1, zebrafish ZP2, variant C; NP_035906.1, mouse ZP3; NP_571406, zebrafish ZP3). **B)** SDS-PAGE of recombinant zebrafish ZP2, ZP3, or ZP2 and ZP3 peptides (6-His mAb, immunoblot) expressed in Sf9 cells after purification from agarose beads. Molecular mass is indicated on the left. **C)** Capacitated mouse sperm binding to beads carrying zebrafish (zf) ZP2, zfZP3 or zebrafish zfZP2 and zfZP3. Beads carrying mouse (m) ZP2 N-termini and beads alone were used as positive and negative controls, respectively. Differential Interference Contrast (DIC) (top) and confocal z projection (bottom) images, sperm nuclei (blue)

stained with Hoechst. **D)** Boxplots represent the median (vertical line) number of mouse sperm binding to mammalian/fish peptide beads or beads alone and data points within the 10th and 90th percentiles (error bars). Boxes include the middle two quartiles, and dots indicate the outliers. Superscript letters show statistical significance ($P<0.05$) defined by One-Way ANOVA followed by Tukey HSD (honestly significant difference) post-hoc test. **E)** Schematic of cross-species insemination assays using mouse sperm to inseminate zebrafish chorion (Top) or eggs (Bottom). **F)** Representative pictures of zebrafish chorion or eggs inseminated with mouse sperm; Top-right panel: mouse sperm binding to normal mouse eggs after 60 min of incubation. Inset, 2.0× magnification. Mouse two-cell embryos serve as a negative control for sperm binding. Bottom-right panel: mouse sperm binding to mouse two-cell embryos; mouse eggs serve as an internal positive control for mouse sperm binding. Top-left panel: mouse sperm incubated with zebrafish chorion without ovulated oocyte (60 min incubation). Bottom-left panel: mouse sperm incubated with zebrafish ovulated oocytes (60 min incubation). **G)** Boxplots represent the median (vertical line) number of mouse sperm binding to mammalian/fish oocytes or embryos (sperm bound per 20 μm^2 projected surface area) and data points within the 10th and 90th percentiles (error bars). Boxes include the middle two quartiles, and dots indicate the outliers. Superscript letters show statistical significance ($P<0.05$) defined by One-Way ANOVA followed by Tukey HSD (honestly significant difference) post-hoc test.

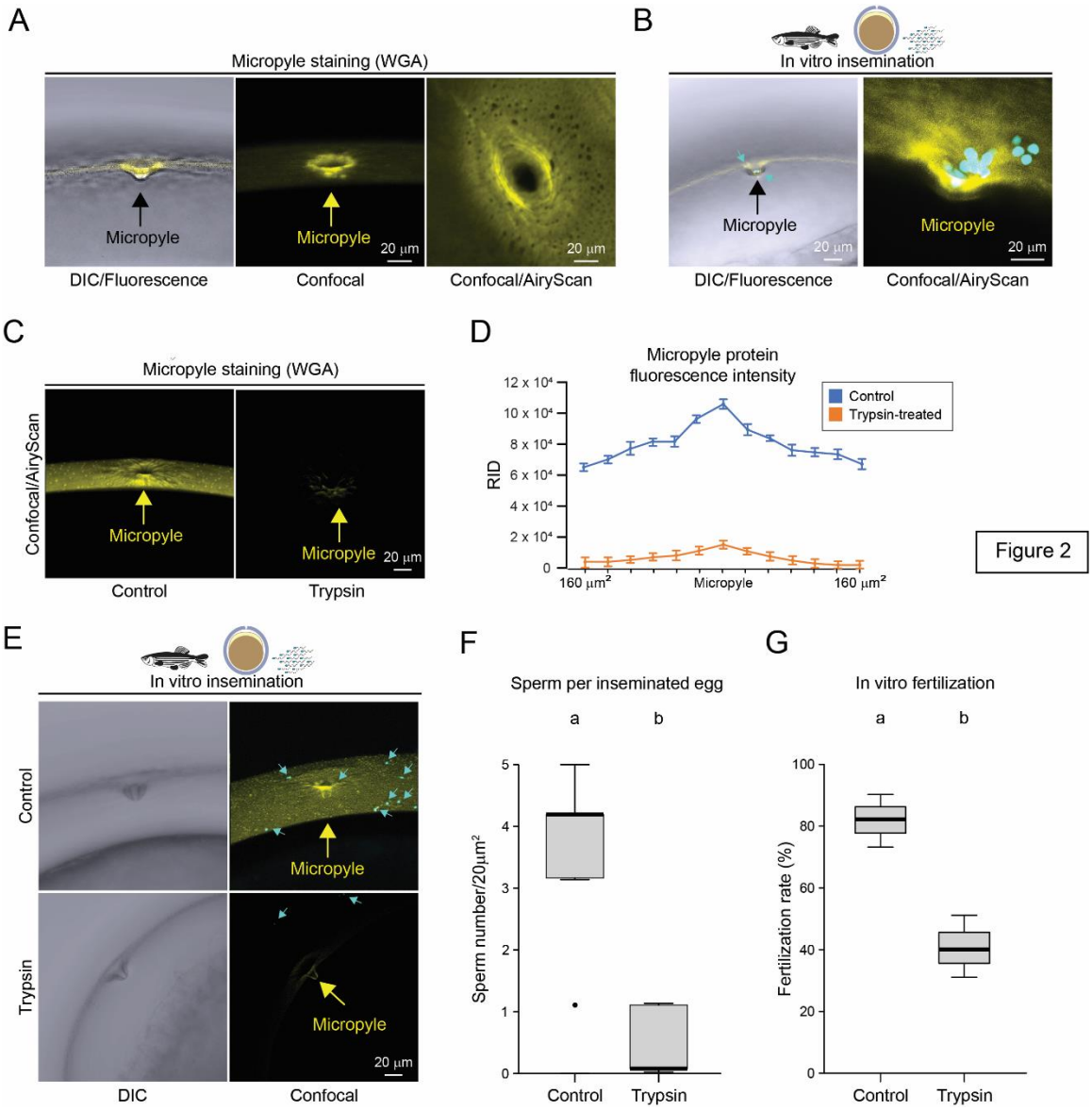

Figure 2. Fish sperm interaction with the micropyle. A) Confocal images of the micropyle stained by WGA-633 in zebrafish oocytes (n >15); arrows indicate the micropyle. **B)** Zebrafish *in vitro* insemination: Hoechst-stained zebrafish sperm (light blue) that have approached or entered the micropyle in freshly ovulated oocytes (yellow, WGA-633-stained); samples were fixed in paraformaldehyde few seconds after insemination. **C)** Zebrafish eggs untreated (left) or treated with trypsin to eliminate the micropyle protein (right). **D)** Fluorescence was measured (Fiji/ImageJ) within a 20 µm2 area; 0 indicates the micropyle opening position (yellow), 160 µm indicates the most distant position measured from micropyle opening. **E)** Same as in (C); left, DIC, right, confocal images (maximum intensity projection) of zebrafish oocytes inseminated with zebrafish sperm. **F)** Same as in 1G, for the quantification of the number of zebrafish

sperm approaching and entering the micropyle of oocytes treated/not treated (control) with trypsin (n = 3). **G)** Same as in 1G, for fertilization rates (n = 3).

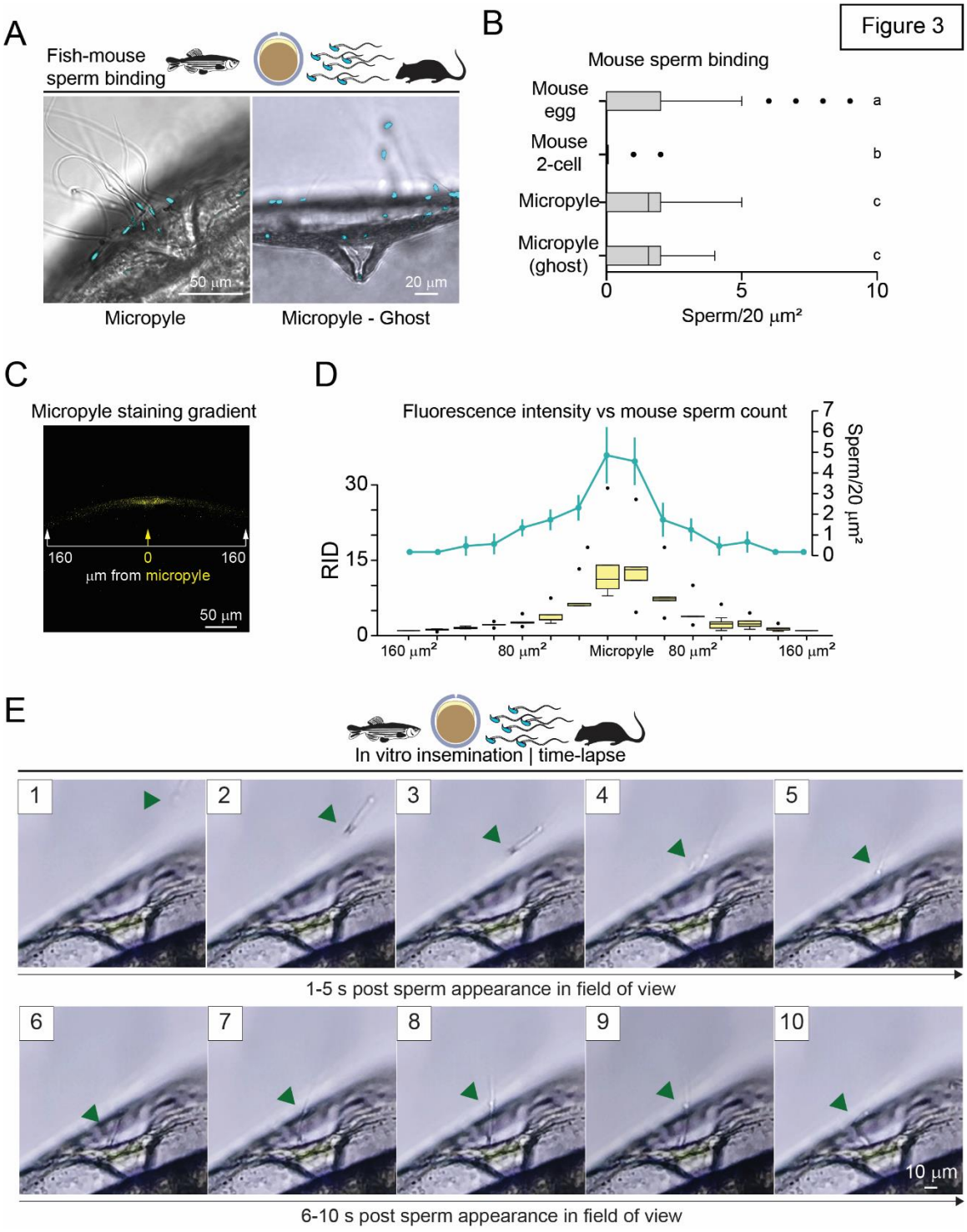

Figure 3. Mouse sperm cross the fish micropyle. A) Cross-species insemination: mouse sperm (Hoechst-stained, light blue) in the zebrafish micropyle region of a chorion (60 min incubation) surrounding the oocyte (left), or of a chorion mechanically freed from the oocyte (right, Ghost). **B)** Quantification of mouse sperm in the micropyle region of chorion with or without zebrafish oocyte: same as 1G; mouse eggs or two-cell

embryos served as an internal positive and negative control for sperm binding (*n* = 3). **C)** X-Y plane confocal projection of zebrafish chorion encompassing the WGA-633 (yellow) micropyle region (~320 µm); bar with arrows indicates positions at which fluorescence was measured (Fiji/ImageJ) as in 2D. **D)** Quantification of mouse sperm across the micropyle region: boxplots represent the median (vertical line) raw integrated density ratio (RID ratio, left Y axis) measured on ten zebrafish VEs; data points within the 10th and 90th percentiles (error bars). Boxes include the middle two quartiles, and dots indicate the outliers. A light blue line represents the number of sperm (right Y axis) found in the corresponding chorion position (X axis); error bars represent s.e.m.; statistical significance ($P<0.05$) across RID ratios or sperm numbers in different positions is defined by One-Way ANOVA followed by Tukey HSD post-hoc test. **E)** Time-lapse frames from supplementary video 1, showing the first sperm entering the micropyle of a freshly ovulated zebrafish egg. Green arrowheads indicate mouse sperm. Insets show the number of seconds ('s') after the first sperm appears in the field of view.

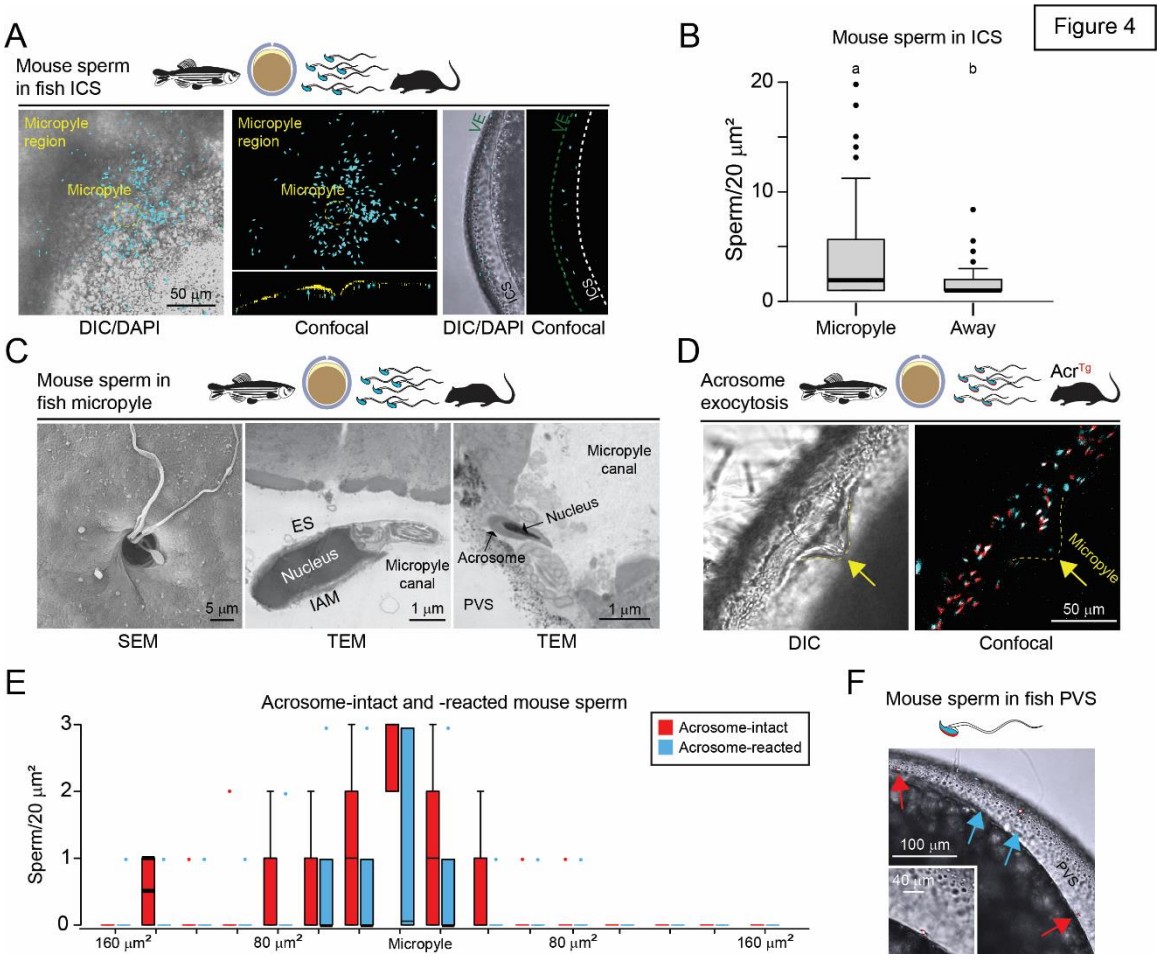

Figure 4. Localization and dynamics of sperm interactions with the micropyle and inter-chorion space in zebrafish oocytes. A) Hoechst-stained sperm (blue) which has crossed the micropyle. DIC (left) and confocal (mid-panel) projection of sperm accumulated in the inter-chorion space (ICS) of a zebrafish oocyte imaged from the top; in the left- and middle/top panels, the 633 channel is turned off to visualize the sperm accumulated in the ICS around the micropyle region (yellow circled); inset shows a longitudinal section of the same oocyte, showing the Hoechst-stained sperm (blue) under the WGA-633-stained micropyle region (yellow). Right, Hoechst-stained sperm (blue) is included in the PVS. **B)** Quantification as in 1D of mouse sperm in the ICS below (left) or away (right) from the micropyle region. Error bars represent s.e.m., statistical significance ($P<0.05$) is defined by One-Way ANOVA followed by Tukey HSD. **C)** Electron microscopy of mouse sperm in the zebrafish micropyle region and within the micropyle canal, 1 hour after insemination. Left, SEM, mid and right panels, TEM; IAM, inner acrosomal membrane. OAM, outer acrosomal membrane; ES, equatorial segment. **D**) Acr^{Tg} sperm in the micropyle region. Left, DIC, right, confocal projection. The yellow arrow indicates the micropyle opening. **E**) As in 1G, with Acr^{Tg} sperm (intact vs. reacted). **F**) Acrosome-intact (red arrows) and reacted (light-blue arrows) mouse sperm in zebrafish ICS. Inset represents a 2x magnification of an acrosome-intact sperm in the ICS.

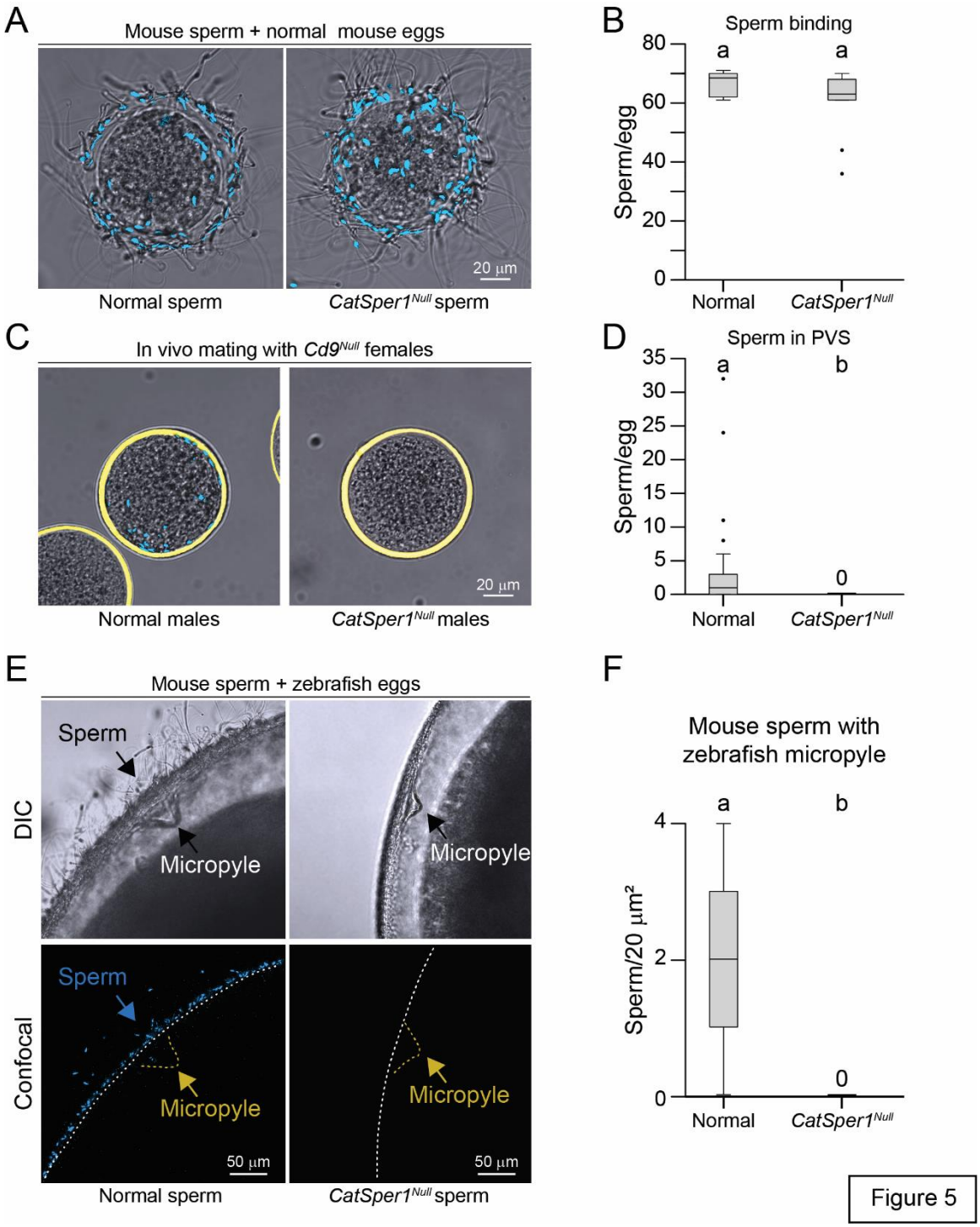

Figure 5. CatSper is necessary for mouse sperm crossing the zebrafish micropyle. A) Hoechst-stained fertile *Catsper1*^{Het} (Normal, left) and *Catsper1*^{Null} sperm binding to ovulated mouse eggs. **B)** Same as in 1D, per mouse egg. **C)** Fertile *Catsper1*^{Het} (Normal, left) and *Catsper1*^{Null} sperm in the PVS of *Cd9*^{Null} female eggs upon *in vivo* mating. **D)** Same as in 1D, number of PVS sperm per *Cd9*^{Null} mouse egg. **E)** Fertile *Catsper1*^{Het}

(Normal, left) and *Catsper1*^{Null} (right) Hoechst-stained sperm in the micropyle region of zebrafish eggs; top, DIC image, bottom, confocal. **F)** Same as in 1G, with normal vs. *Catsper1*^{Null} sperm.

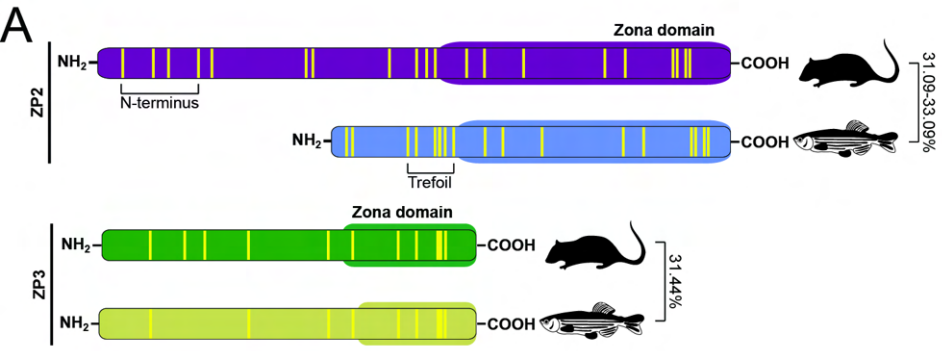
A
Zona domain
NH2
COOH
ZP2
N-terminus
Trefoil
31.09-33.09%
ZP3
31.44%

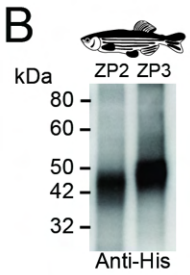
B
kDa
ZP2 ZP3
80
60
50
42
32
Anti-His

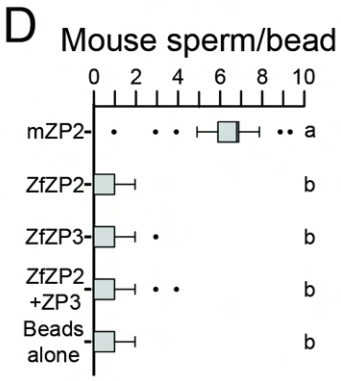
D
Mouse sperm/bead
0 2 4 6 8 10
mZP2
ZfZP2
ZfZP3
ZfZP2 +ZP3
Beads alone
a
b
b
b
b

C
mZP2
zfZP2
zfZP3
zfZP2+ZP3
Beads alone
50 µm
40 µm
Mouse sperm

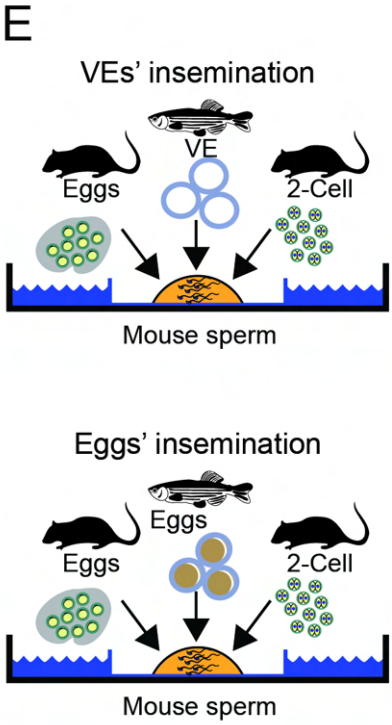
E
VEs' insemination
VE
Eggs
2-Cell
Mouse sperm
Eggs' insemination
Eggs
Eggs
2-Cell
Mouse sperm

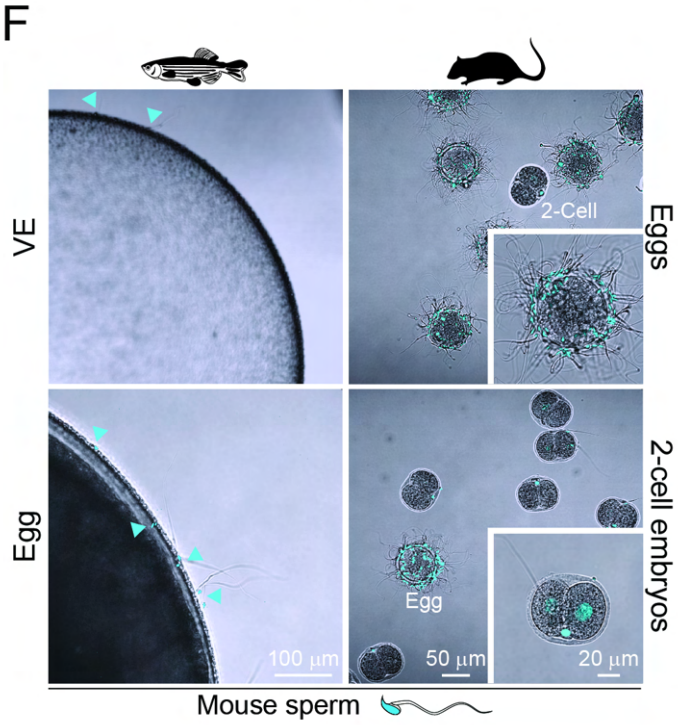
F
VE
Egg
Eggs
2-cell embryos
2-Cell
Egg
100 µm
50 µm
20 µm
Mouse sperm

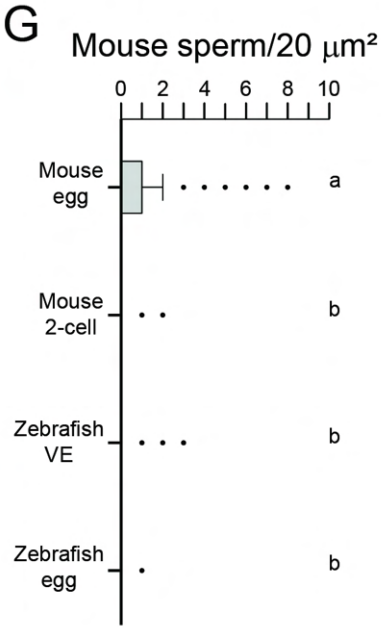
G
Mouse sperm/20 µm²
0 2 4 6 8 10
Mouse egg
Mouse 2-cell
Zebrafish VE
Zebrafish egg
a
b
b
b

Figure 1

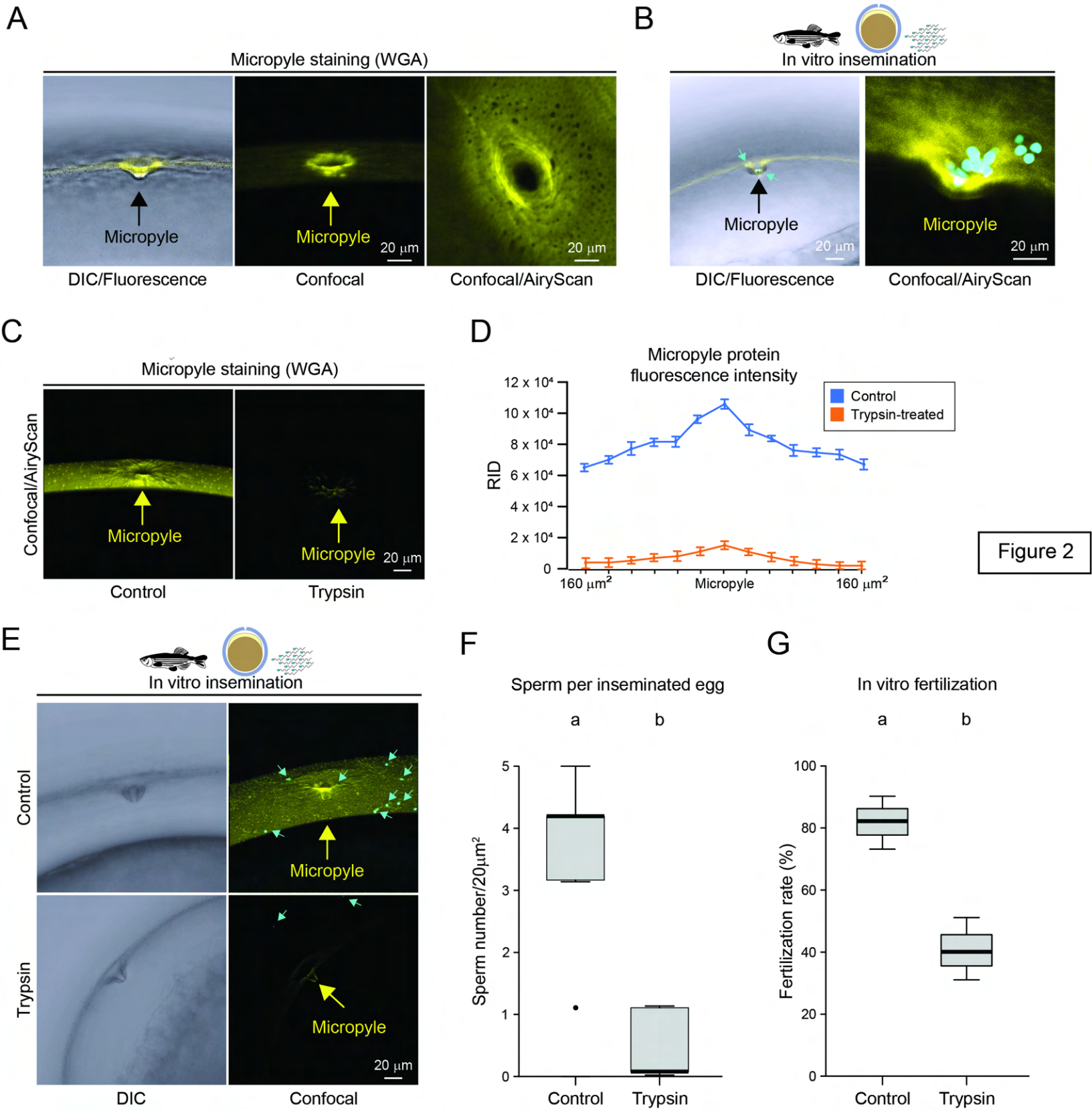
A
Micropyle staining (WGA)
Micropyle
Micropyle
20 µm
20 µm
DIC/Fluorescence
Confocal
Confocal/AiryScan
B
In vitro insemination
Micropyle
20 µm
Micropyle
20 µm
DIC/Fluorescence
Confocal/AiryScan
C
Micropyle staining (WGA)
Confocal/AiryScan
Micropyle
Micropyle
20 µm
Control
Trypsin
D
Micropyle protein fluorescence intensity
Control
Trypsin-treated
RID
12 x 10⁴
10 x 10⁴
8 x 10⁴
6 x 10⁴
4 x 10⁴
2 x 10⁴
0
160 µm²
Micropyle
160 µm²
Figure 2
E
In vitro insemination
Control
Trypsin
Micropyle
Micropyle
20 µm
DIC
Confocal
F
Sperm per inseminated egg
a
b
Sperm number/20µm²
5
4
3
2
1
0
Control
Trypsin
G
In vitro fertilization
a
b
Fertilization rate (%)
100
80
60
40
20
0
Control
Trypsin

Figure 3

A

Fish-mouse sperm binding

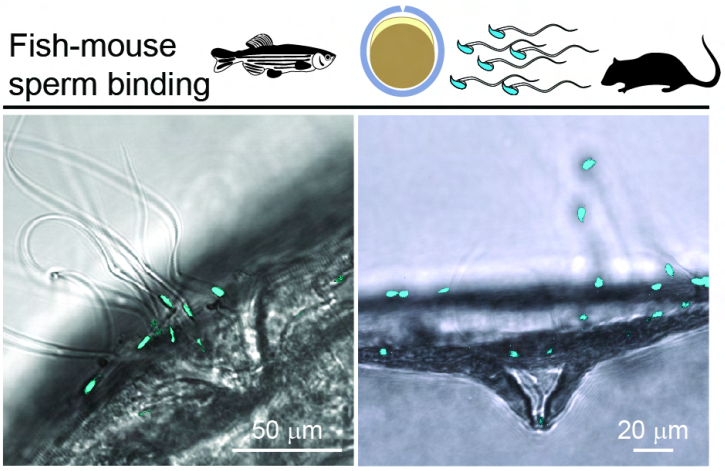

Micropyle | Micropyle - Ghost

B

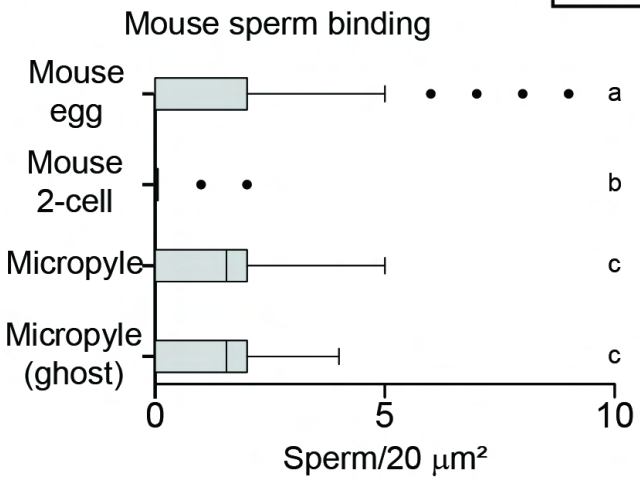

C

Micropyle staining gradient

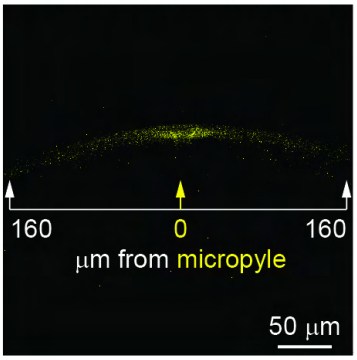

D

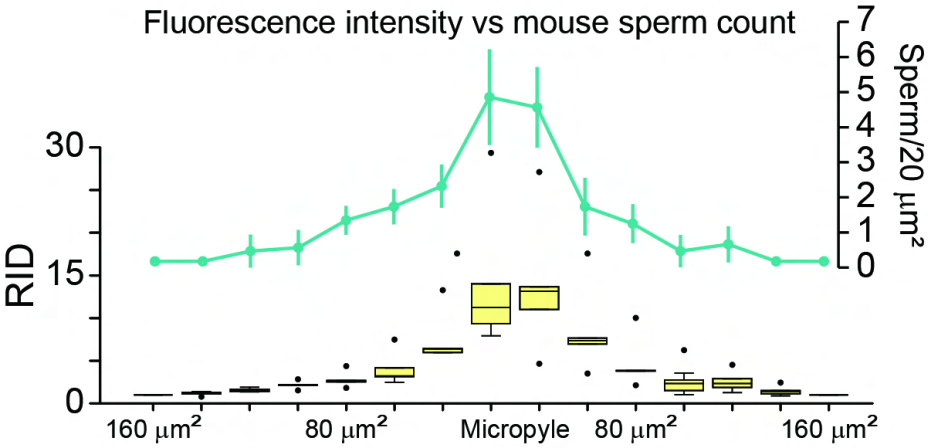

E

In vitro insemination | time-lapse

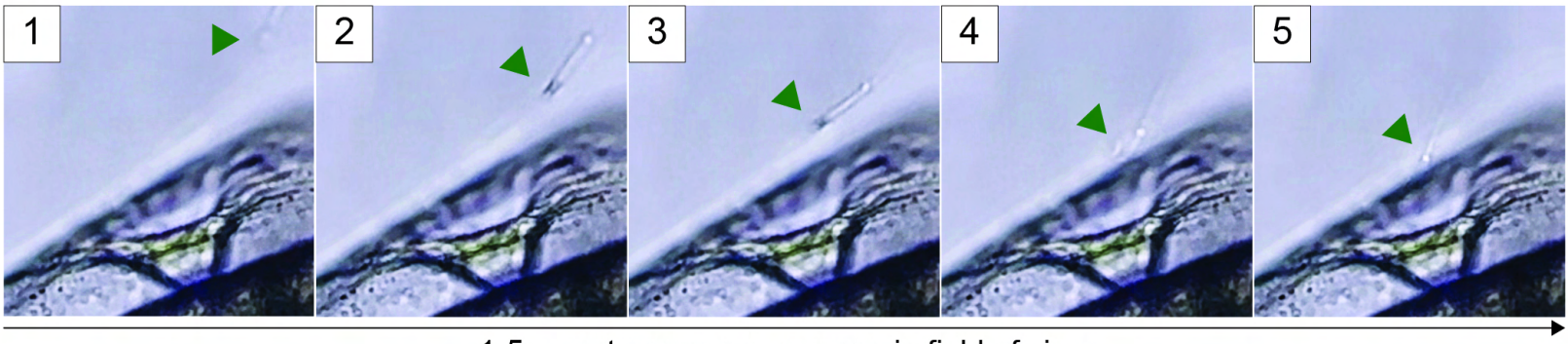

1-5 s post sperm appearance in field of view

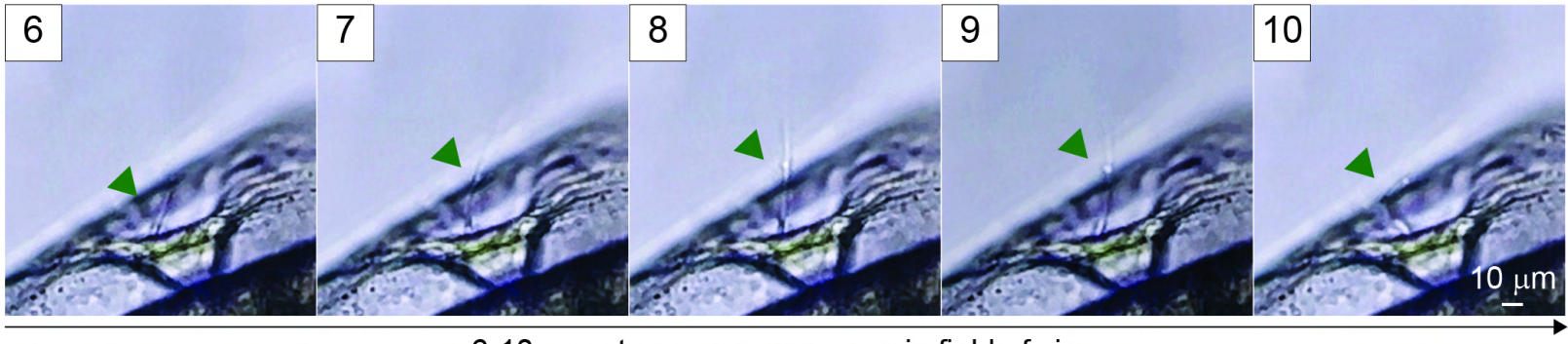

6-10 s post sperm appearance in field of view

Figure 4

A

Mouse sperm in fish ICS

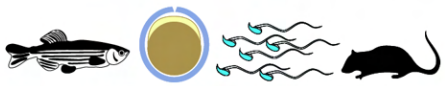

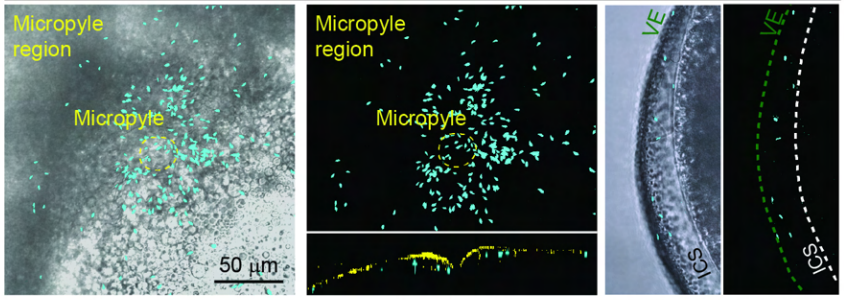

DIC/DAPI Confocal DIC/DAPI Confocal

B

Mouse sperm in ICS

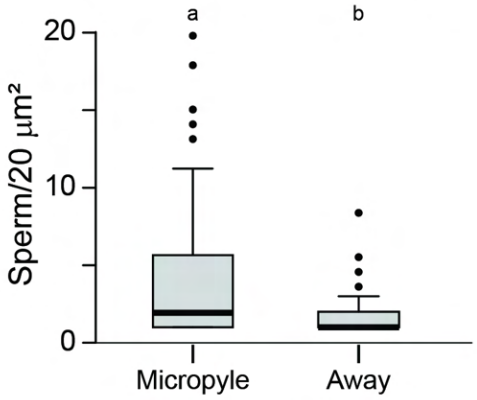

C

Mouse sperm in fish micropyle

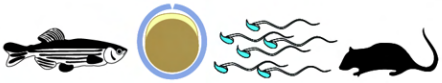

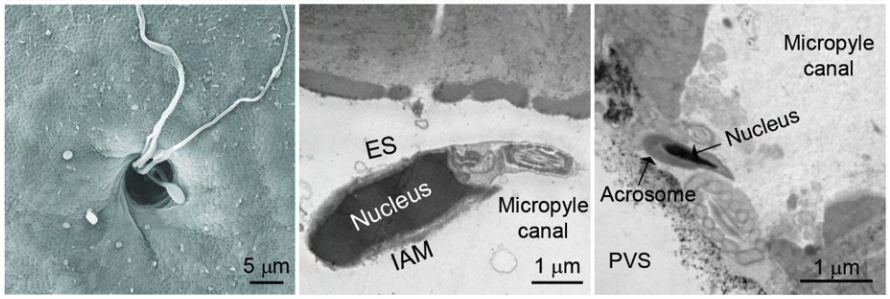

SEM TEM TEM

D

Acrosome exocytosis

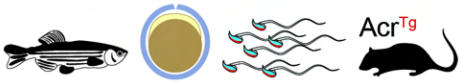

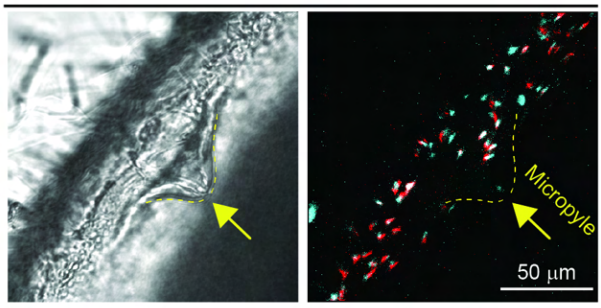

DIC Confocal

E

Acrosome-intact and -reacted mouse sperm

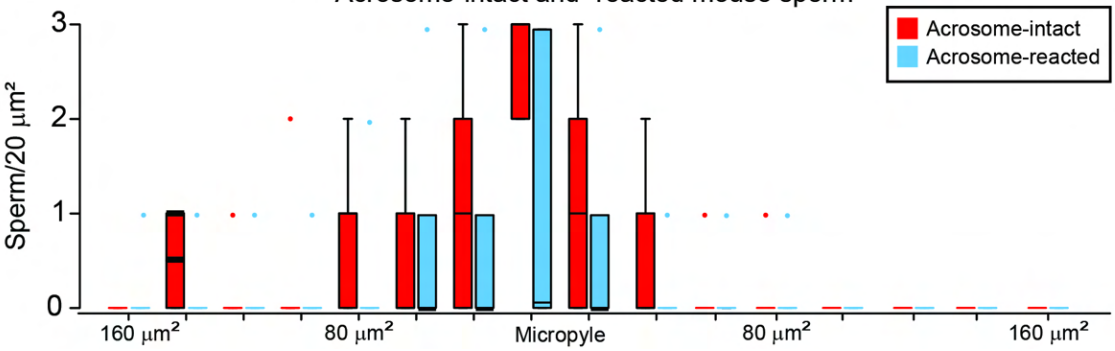

F

Mouse sperm in fish PVS

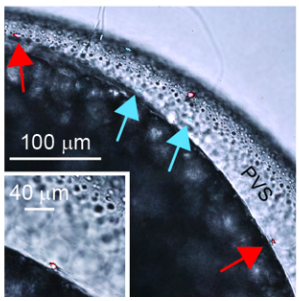

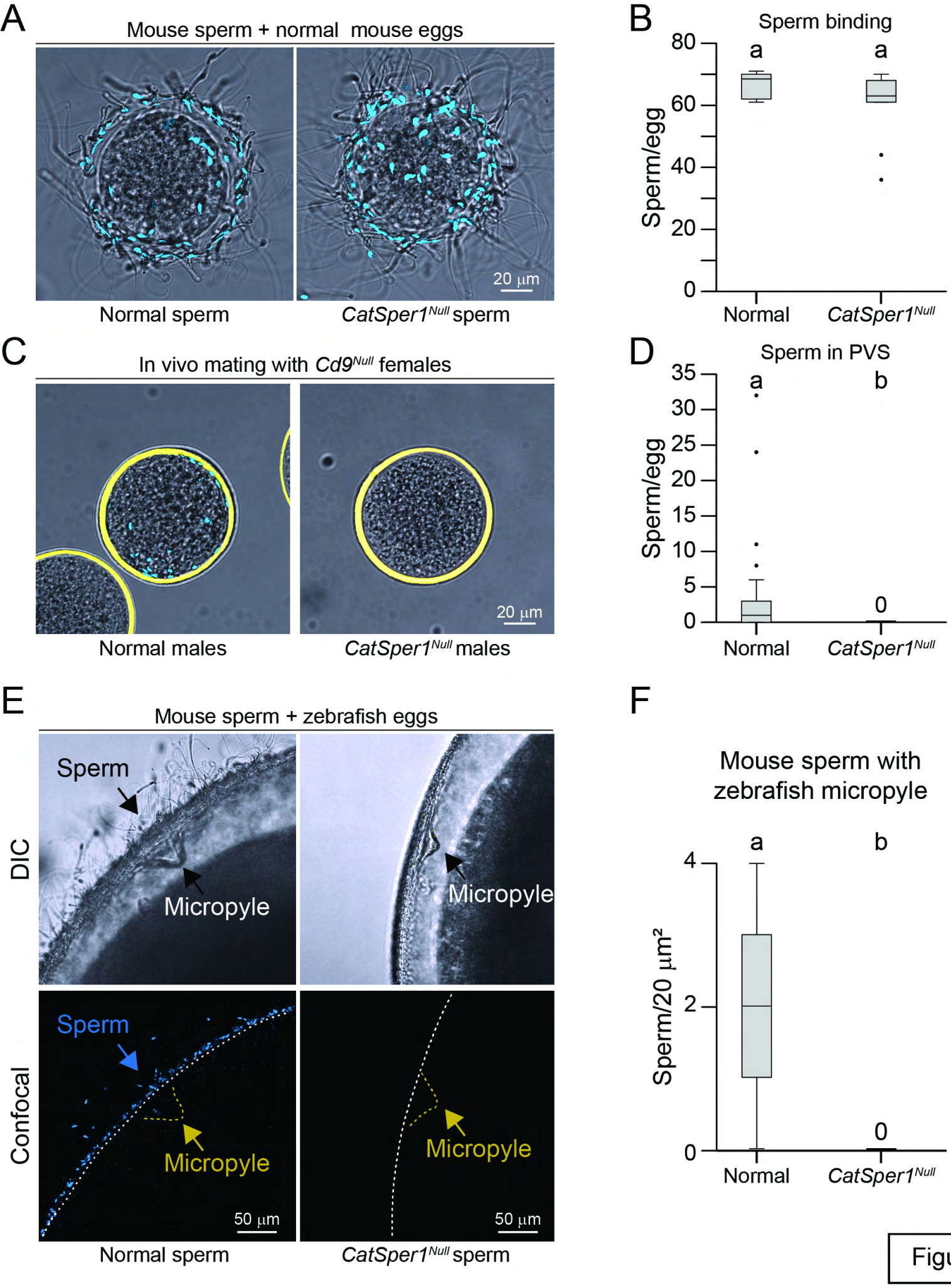
A
Mouse sperm + normal mouse eggs
20 µm
Normal sperm
CatSper1Null sperm
B
Sperm binding
Sperm/egg
80
60
40
20
0
a
a
Normal
CatSper1Null
C
In vivo mating with Cd9Null females
20 µm
Normal males
CatSper1Null males
D
Sperm in PVS
Sperm/egg
35
30
25
20
15
10
5
0
a
b
0
Normal
CatSper1Null
E
Mouse sperm + zebrafish eggs
DIC
Confocal
Sperm
Micropyle
Micropyle
Sperm
Micropyle
Micropyle
50 µm
50 µm
Normal sperm
CatSper1Null sperm
F
Mouse sperm with zebrafish micropyle
Sperm/20 µm²
4
2
0
a
b
0
Normal
CatSper1Null

Figure 5